Using Landslide Statistical Index Technique for Landslide Susceptibility Mapping: Case Study: Ban Khoang Commune, Lao Cai Province, Vietnam

Long Nguyen Thanh [1], Yao-Min Fang [2,*], Tien-Yin Chou [2] (ID), Thanh-Van Hoang [2] (ID), Quoc Dinh Nguyen [1] (ID), Chen-Yang Lee [3], Chin-Lun Wang [3], Hsiao-Yuan Yin [3] and Yi-Chia Lin [3]

1   Vietnam Institute of Geosciences and Mineral Resources, 67 Chien Thang Rd, Van Quan Street, Ha Dong, Hanoi 100000, Vietnam
2   Geographic Information System Research Center, Feng Chia University, 100 Wenhwa Rd, Seatwen, Taichung City 40724, Taiwan
3   Soil and Water Conservation Bureau, Council of Agriculture, No 6, Guanghua Rd, Nantou City 540206, Taiwan
*   Correspondence: frankfang@gis.tw; Tel.: +886-4-24516609

Abstract: Ban Khoang is a mountainous commune in Sa Pa district located in the central part of Lao Cai province, Vietnam. Landslides occur frequently in this area and seriously affect the local living conditions. To help the local authority in developing a landslide disaster action plan, the statistical index method for landslide susceptibility mapping is applied. As the result, the landslide susceptibility zonation (LSZ) map was created. The LSZ map indicates that areas of low, moderate, high and very high landslide susceptibility zones are, respectively, 20.3 km^2, 12.4 km^2, 15.4 km^2, and 5.2 km^2; most of the observed landslide areas that are well predicted belong to high or very high landslide susceptibility classes. In detail, 80% observed landslide areas and 78.57% number of observed landslides were well predicted, and the area (AUC) under the receiver operating characteristic (ROC) curve obtained 80.3%. Hence, the high and very high landslide susceptibility classes in the LSZ map can be considered highly believable, and the LSZ map will be reliable to use in the practice.

Keywords: natural hazards; landslide; susceptibility; GIS; Vietnam

1. Introduction

Ban Khoang is a mountainous commune in Sa Pa district, Lao Cai province of Vietnam, where these landslides occur regularly (Figure 1). In particular, a vast landslide happened in Can Ho A village, Ban Khoang commune in September 2013, causing 14 people loss and severe property damage. Hence, predicting landslide hazards is very important for the inhabitants and local administration of Ban Khoang commune to mitigate landslide damage in this area.

According to the result of a nationwide project "Investigation, assessment and geohazards susceptibility zonation in mountainous areas of Vietnam" [1] recently, Ban Khoang is one of 200 communes with highest level of landslides susceptibility in Vietnam.

Therefore, the LSZ mapping will be very necessary and helpful for local authorities and people in landslide hazard prevention and mitigation, as well as developing a landslide action plan. In addition, the LSZ map will be a technical foundation for practical activities relevant to setting up landslide early warning systems.

The most straightforward initial approach to any study of landslide hazards is the compilation of a landslide inventory and analyzing the relationship with different causative factors to predict landslide-prone areas [2]. In Ref. [3], Carrara (1983) introduced the so-called statistical approach for landslide hazard assessment. This technique has been widely employed and has become one of the most popular approaches for landslide hazard

assessment worldwide. Combinations of factors that have led to landslides in the past are identified statistically, and quantitative predictions are made for areas currently free of landslides but with similar conditions. Since then, many other statistical approaches have been proposed and used in landslide susceptibility mapping and analyses.
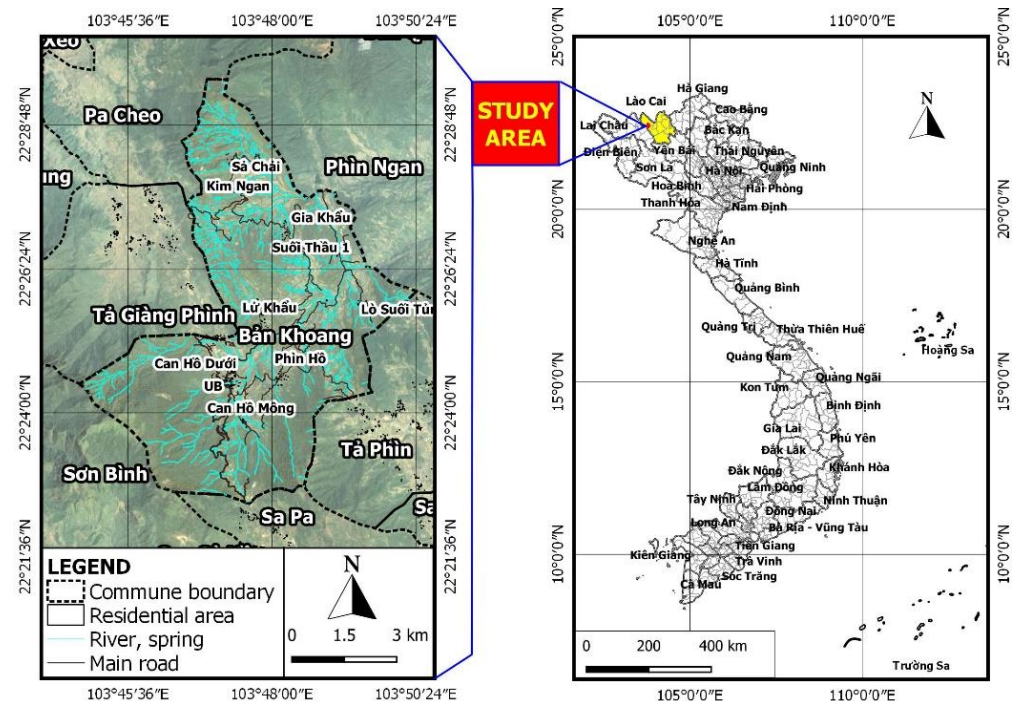
Figure 1. In this study area, 28 landslides, covering 0.262 km^2 (Figure 2), were identified (from 2012 up to May 2022) based on (1) field recognizance to investigate landslide occurrences, (2) collection of historical literature on landslides, and (3) interpretation of available multi-serial google images coupled with field verification.

Basically, statistical landslide susceptibility approaches are based on related spatial information on past landslide activities (i.e., landslide presence/absence) to static geoenvironmental factors (e.g., topography, geology, geomorphology, land use, fault density, soil, and drainage density) using statistical techniques. In Ref. [4], Steger et al. (2016) commented that the generated empirical relation, commonly expressed as a relative susceptibility score, is then applied to each spatial unit of an area (e.g., grid cell, and slope unit) [5–7]. The validation of spatial predictions is commonly evaluated by interpreting inventory-based predictive performance estimates [8–10].

It is obvious that the landslide inventory is a vital component to obtaining high-quality statistical landslide susceptibility models because most analysis steps are dependent on a correct representation of past landslide occurrences [4,9,11–14].

Several studies compared statistical landslide susceptibility models produced from heterogeneous inventories [4,15–19]. However, a differentiated evaluation of the propagation of potential inventory-based errors into landslide susceptibility models was hampered due to the practical inseparability of positional accuracy and inventory completeness as well as the lack of truly accurate reference inventories.

There are many previous works using the statistical approaches for landslide susceptibility assessment (e.g., methods of statistical index, certainty factor, probability, weight of evidence modeling, and logistic regression). However, the selection of input parameters or causative factors for landslide susceptibility mapping, the method for landslide susceptibility mapping and landslide susceptibility index classification are still confused between many studies.

The statistical index method is considered the simplest and quantitatively suitable method for statistical approaches for landslide susceptibility mapping. However, it has been adopted by various researchers [19–27].

Therefore, in this study, the statistical index method is applied for landslide susceptibility analyses of Ban Khoang commune in Sa Pa district, Lao Cai province of Vietnam. The research result will play an important role for landslide hazard prevention and mitigation in this mountainous commune in Vietnam.
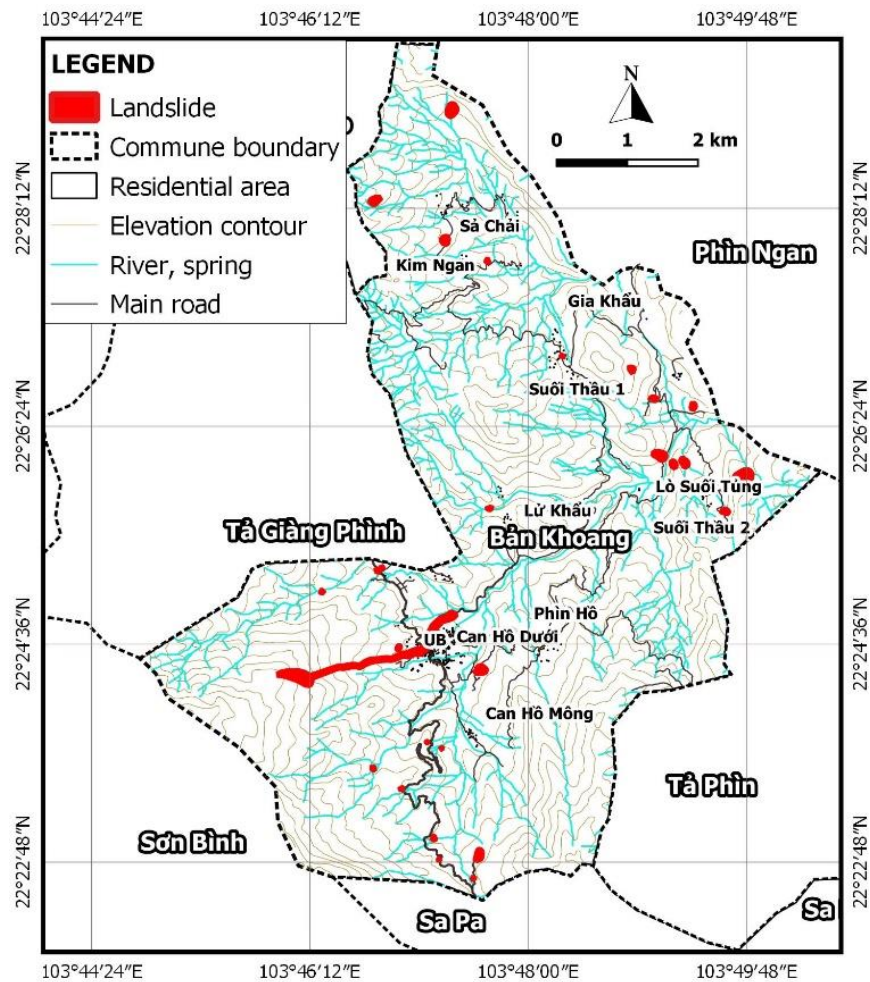
Figure 2. Map of landslide inventory in the study area.

2. Landslide Inventory

The study area, Ban Khoang commune selected for assessment of landslides susceptibility (Figure 1) is about 53.3 km^2.

The average size of the landslides in the study area is approximately 9369 m^2, but the details about width, depth, types, or causes of some landslides were not identified. Some pictures of landslide inventory are displayed in Figure 3.

(**A**)

(**B**)

(**C**)

Figure 3. Some landslide pictures in Ban Khoang commune, Sa Pa district, Lao Cai province of Vietnam. (**A**) Landslide as debris flow occurred near hospital of Ban Khoang commune in 2013. (**B**) Landslides near provincial road 155 in Ban Khoang commune. (**C**) Landslide on the provincial road 155, the section closed to Can Hồ B village in Ban Khoang commune on 22 May 2022.

3. Landslide Causative Factors

The selection of causative factor maps for landslide susceptibility should be considered carefully based on relevance, availability and scale attributes. These are cumbersome in Vietnam, as systematic studies and inventories of spatial characteristics and land cover features have only been initiated recently by different government institutions. Therefore, such data are often lacking, incomplete, or on a scale that is not useful for scientific purposes, especially in remote and rural regions as the present study area. Ham-

pered by such constraints, eight digital causative factors map for landslide analysis could be developed:

- Topography is intrinsically associated with landslides by slope gradient and other factors, such as weathering, precipitation, soil thickness, etc. Hence, topography strongly affects landslides [28,29]. Ban Khoang is a mountainous area where the microclimate is quite predominant. Hence, the aspect is considered an indirect landslide causative factor in this study. A digital elevation map (DEM) of the study area with a pixel size of 10 m by 10 m was obtained by using inverse distance weighted interpolation in QGIS 3.6 from elevation points and contours of a topographic map, scale 1:10,000, published by the Cartographic Publishing House, Vietnamese Ministry of Natural Resources and Environment (2019). Then the aspect map of Ban Khoang commune (Figure 4A) was developed based on the Aspect tool inside QGIS 3.6 software.
- In most landslide studies, slope gradient is considered a principal causative or triggering factor. A slope map was derived from the DEM using the slope function tool of QGIS 3.6. The slope map is in the form of a raster map with the same 10 m pixel size as the DEM, but was converted to vector by separating the slope angles into six classes: (1) flat-gentle slope (<5°), (2) fair slope (5–15°), (3) moderate slope (15–25°), (4) fairly moderate slope (25–35°), (5) steep slope (35–45°), and (6) very steep slope (>45°). The map of slope classes of Ban Khoang commune is displayed in Figure 4B.
- Geology and slope instability are strongly associated [30,31]. Hence, a geological map of Ban Khoang (Figure 4C) was derived from the map of geology and mineral resources of the Lao Cai sheet group, scale 1:50,000 by Lap et al. (2003) [32]. Figure 4C displays the distribution of geological classes in Ban Khoang commune in Sa Pa district, Lao Cai province of Vietnam.
- Geomorphology is considered an essential factor related to landslide occurrence in the study area. Based on the analyses of the topological characteristics, geological structures, neotectonic movements, and morphometries, six geomorphological units can be identified in the study area by [33] (Figure 4D).
- Soil is an essential factor of slope instability in many settings [34,35]. A digital map of soil was derived from previous work in Lao Cai province carried out by the National Institute of Agriculture Planning and production (2019), identifying three types of soil mechanics in the study area, i.e., (1) outcrop, (2) reddish-yellow humus soil on claystone, and (3) reddish-yellow humus soil on magma rocks (Figure 4E). The soil depth map (Figure 4F) was derived based on the soil depth information based on the map of soil mechanics.
- Neotectonics contribute to slope instability by fracturing, faulting, jointing, and deforming foliation structures [36,37]. For this study, faults were extracted from the map of geology and mineral resources scale 1:50,000. Additionally, lineaments were interpreted from free available Landsat 8 captured by NASA in 2020. The fault and lineament density was calculated as the total length of faults and lineament per 1 km^2 (See Figure 4G).
- Studies have shown that the proximity to drainage axes with intensive gully erosion is an important factor controlling the occurrence of landslides [38,39]. A map of river density was derived on the basis of the digitizing river and stream courses on the topographic map and interpolation in QGIS software (version 3.6). A map of the river density class (Figure 4H) was created by subdividing the river density range values into five classes: (1) <1000 m/km^2, (2) 1000–2000 m/km^2, and (3) 2000–3000 m/km^2, (4) 3000–4000 m/km^2, and (5) >4000 m/km^2.
- Vegetation augments slope stability primarily in two ways: (1) by removing soil moisture through evapotranspiration and (2) by providing root cohesion to the soil mantle [40]. A land-use map was obtained from the land-use map of Lao Cai published by the land administration department of the Ministry of Natural Resources and Environment, 2019 [41]. The land use composed of 10 land-use classes is displayed in Figure 4I.

(**A**) Aspect map.

(**B**) Slope map.

(**C**) Geological map.

(**D**) Geomorphological map.
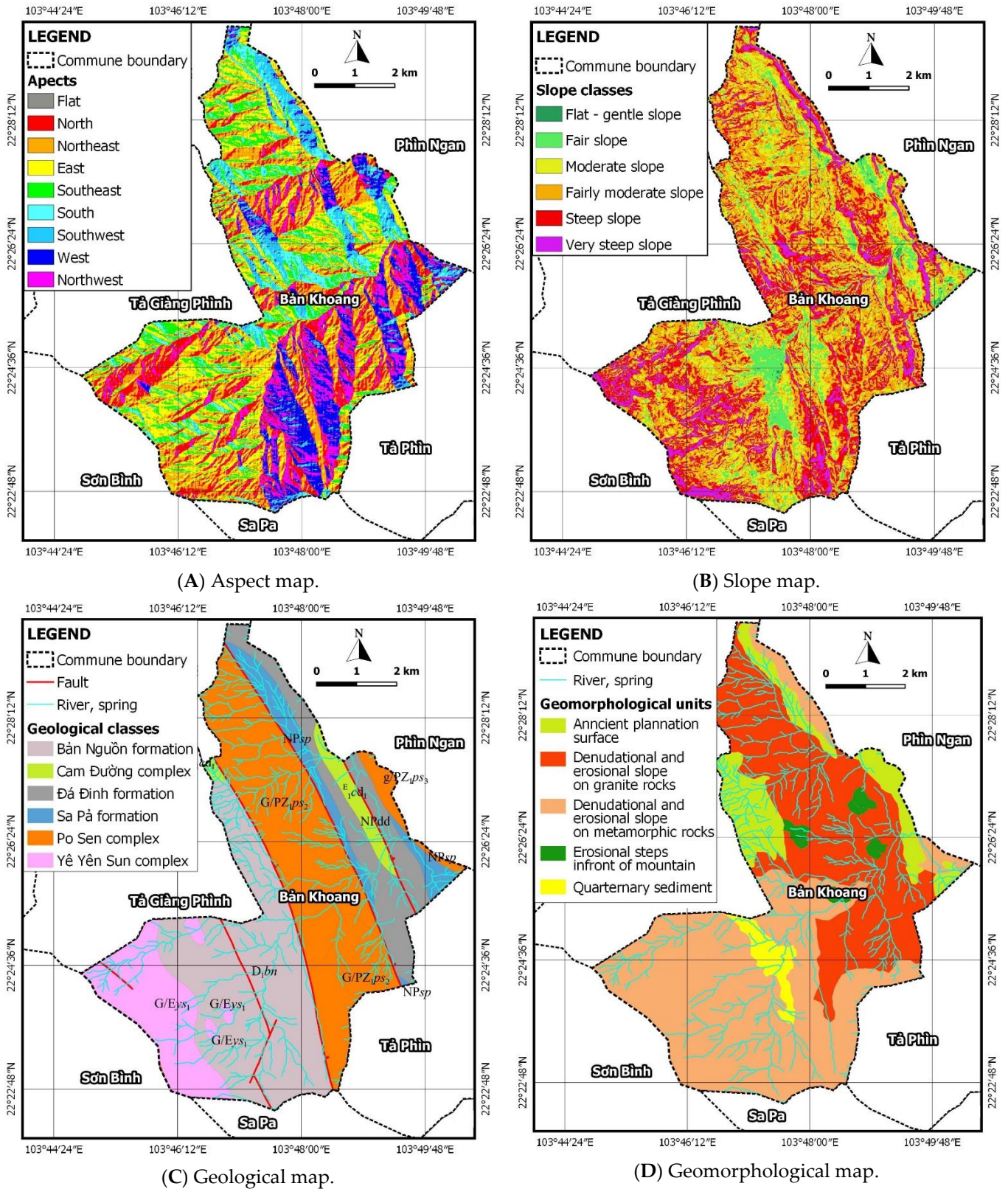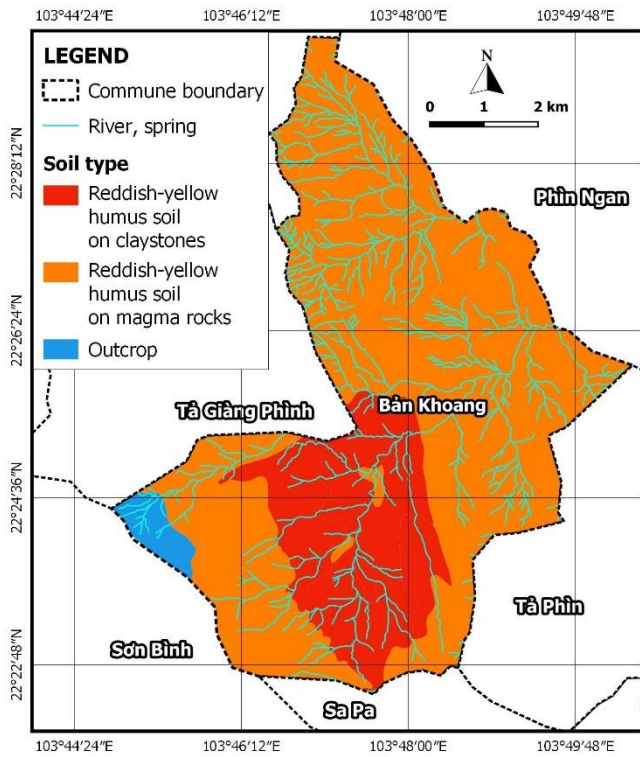
Figure 4. *Cont.*

(**E**) Soil-type map.
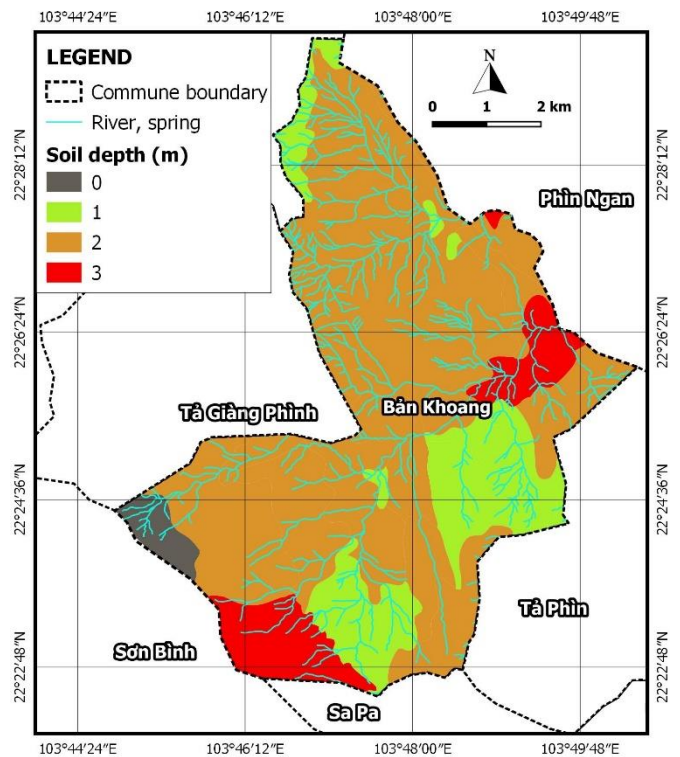
(**F**) Soil-depth map.
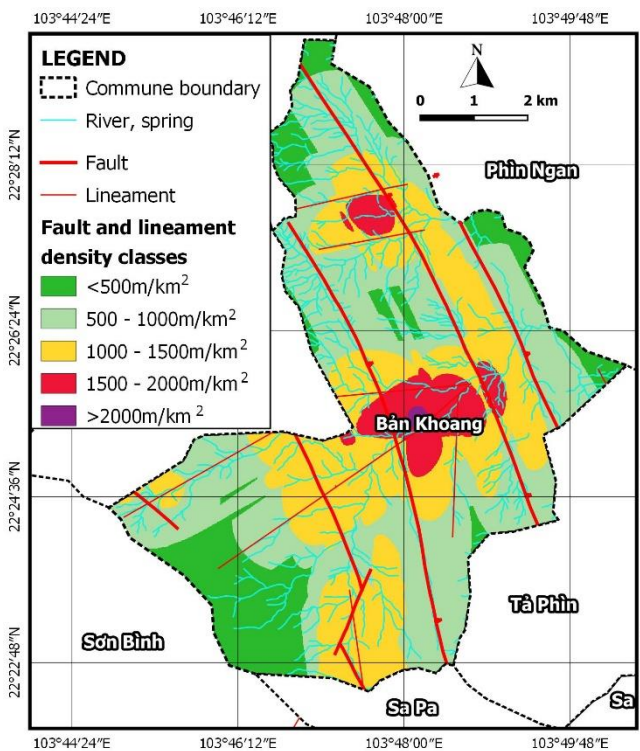
(**G**) Map of fault and lineament density.
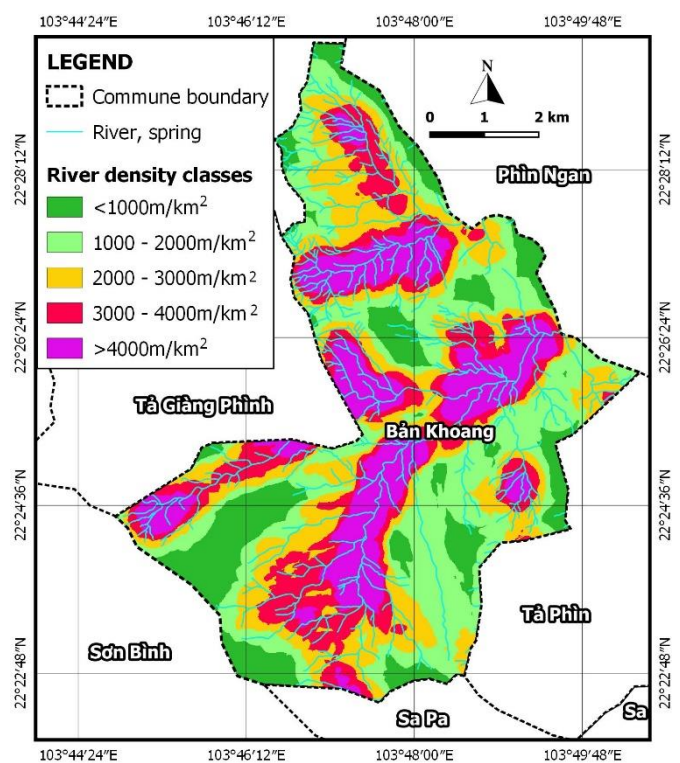
(**H**) Map of river density.

Figure 4. *Cont*.
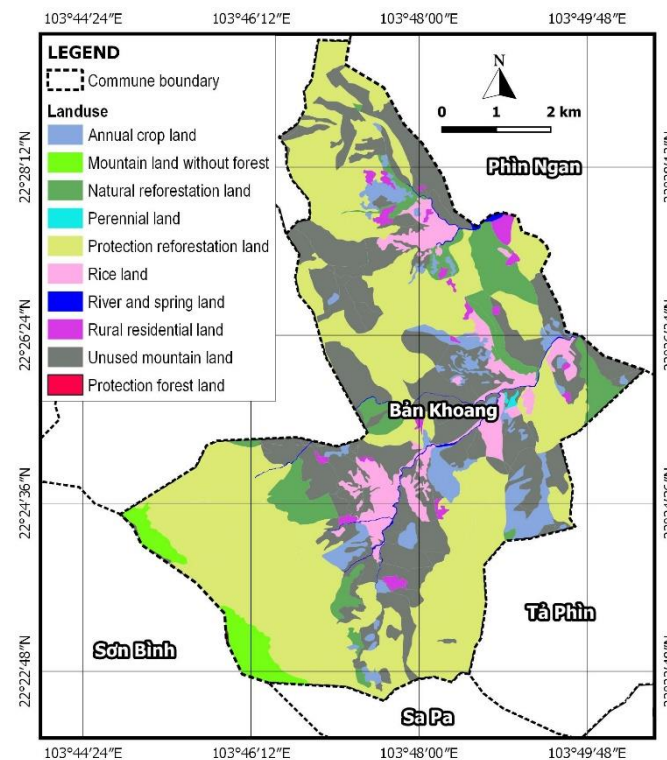
(**I**) Land-use map.

Figure 4. Landslide causative parameters for landslide susceptibility mapping of Ban Khoang commune.

4. Method for Landslide Susceptibility Analysis

The statistical index method is a bivariate statistical technique introduced by van Westen in 1997 [20] for landslide susceptibility analyses. Other researchers, such as Gebremedhin et al., 2021 [21], Mandal et al., 2018 [22], Wu et al., 2017 [23], Wang et al., 2016 [24], Dieu et al., 2011 [25], Long, 2008 [19], Cevik and Topal, 2003 [27], and Oztekin and Topal, 2005 [26], also applied this technique and termed it the statistical index method. In the statistical index method, a weight value for a parameter class is defined as the natural logarithm of the landslide density in the class divided by the landslide density in the entire map [20].

$$W_{ij} = \ln\left(\frac{f_{ij}}{f}\right) \tag{1}$$

where W_{ij} is the weight of a class i of parameter j, f_{ij} the landslide density within the class i of parameter j, and f the landslide density within the entire map. Hence, the statistical index method is based on statistical correlation of the landslide inventory map with attributes of different parameter maps. The W_{ij} value in Equation (1) is only calculated for classes that have landslide occurrences. If there are no landslide occurrences in a parameter class, the W_{ij} will be assigned to zero [20,30]. This also means that the parameter class having no landslide occurrences will have no correlation with the landslide inventory. Hence, it does not influence the calculation of the landslide susceptibility index.

In this study, nine landslide causative factors, i.e., (1) slope, (2) geology, (3) geomorphology, (4) soil depth, (5) soil type, (6) land use, (7) fault and lineament density, and (8) river density (Figure 4), were used as the layer input for landslide susceptibility index mapping. The workflow for landslide susceptibility mapping in Ban Khoang commune is shown in Figure 5. Every parameter map is crossed with the landslide map, and the density of the landslide in each class is calculated. The distribution of landslides for various data layers and weight wij values are shown in Table 1. The distribution of landslides for

various data layers, weight of class (W_{ij}) of all the causative factors in the study area is displayed in Table 2.
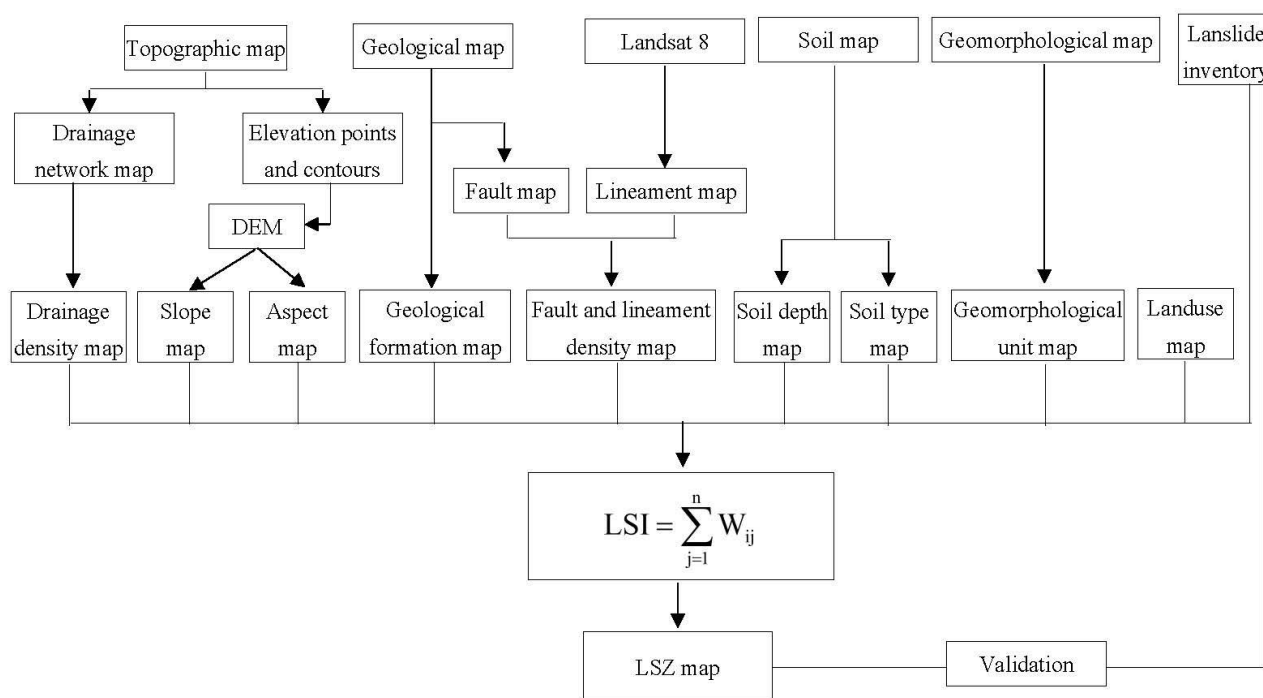
Figure 5. Work flow for landslide susceptibility mapping in the study area.

Table 1. Distribution of landslides for various data layers, weight of class (W_{ij}) of all causative factors in the study area.

Landslide Causative Factors	Landslide Occ. Pixels	% Occ.	No. of Pixels in Domain	% Domain	W_{ij}
Slope					
<5°	11	0.42	2798	0.52	−0.2261
5–15°	537	20.43	45,087	8.46	0.8823
15–25°	580	22.07	114,691	21.51	0.0257
25–35°	508	19.33	182,665	34.26	−0.5723
35–45°	609	23.17	138,605	25.99	−0.1149
>45°	383	14.57	49,356	9.26	0.4539
Fault and lineament density					
<500 m/km^2	348	13.24	81,710	15.32	−0.1461
500–1000 m/km^2	1103	41.97	235,319	44.13	−0.0502
1000–1500 m/km^2	1170	44.52	178,785	33.53	0.2835
1500–2000 m/km^2	7	0.27	35,889	6.73	−3.2296
>2000 m/km^2	0	0.00	1499	0.28	0.0000
River density					
<1000 m/km^2	758	28.84	86,095	16.15	0.5802
1000–2000 m/km^2	603	22.95	135,804	25.47	−0.1044
2000–3000 m/km^2	684	26.03	113,416	21.27	0.2018
3000–4000 m/km^2	250	9.51	96,950	18.18	−0.6478
>4000 m/km^2	333	12.67	100,937	18.93	−0.4014
Soil depth					
0 m	0	0.00	11,686	2.19	0.0000
1 m	175	6.66	94,253	17.68	−0.9763
2 m	2314	88.05	376,835	70.67	0.2198
3 m	139	5.29	50,428	9.46	−0.5812

Table 1. *Cont.*

Landslide Causative Factors	Landslide Occ. Pixels	% Occ.	No. of Pixels in Domain	% Domain	W$_{ij}$
Soil type					
Reddish-yellow humus soil on magma rocks	1629	61.99	401,940	75.38	−0.1957
Outcrop	0	0.00	11,686	2.19	0.0000
Reddish-yellow humus soil on claystone	999	38.01	119,576	22.43	0.5277
Geomorphology					
Ancient planation surface	93	3.54	59,101	11.08	−1.1417
Denudational and erosional slope on metamorphic rocks	1597	60.77	193,797	36.35	0.5140
Denudational and erosional slope on granite rocks	489	18.61	256,604	48.13	−0.9502
Quaternary sediment	427	16.25	9101	1.71	2.2533
Erosional steps in front of mountain	22	0.84	14,599	2.74	−1.1850
Geology					
Sa Pả formation	262	9.97	32,774	6.15	0.4836
Cam Đường formation	169	6.43	15,573	2.92	0.7893
Yê Yên Sun complex	571	21.73	69,501	13.03	0.5110
Po Sen complex	163	6.20	183,843	34.48	−1.7154
Đá Đinh formation	312	11.87	64,195	12.04	−0.0140
Bản Nguồn formation	1151	43.80	167,316	31.38	0.3334
Landuse					
Protection reforestation land	1089	41.44	252,972	47.44	−0.1353
Rice land	241	9.17	29,879	5.60	0.4926
Annual crop land	2	0.08	33,860	6.35	−4.4242
Natural reforestation land	585	22.26	39,883	7.48	1.0906
Rural residential land	16	0.61	8229	1.54	−0.9302
Unused mountain land	682	25.95	152,292	28.56	−0.0958
Mountain land without forest	0	0.00	12,683	2.38	0.0000
Perennial land	0	0.00	619	0.12	0.0000
River and spring land	13	0.49	2660	0.50	−0.0085
Protection forest land	0	0.00	125	0.02	0.0000
Aspect					
Flat	0	0.00	24	0.00	0.0000
North	422	16.06	80,933	15.18	0.0563
Northeast	904	34.40	103,501	19.41	0.5722
East	586	22.30	102,496	19.22	0.1484
Southeast	285	10.84	64,916	12.17	−0.1157
South	100	3.81	40,339	7.57	−0.6872
Southwest	102	3.88	33,324	6.25	−0.4764
West	58	2.21	54,362	10.20	−1.5303
Northwest	171	6.51	53,307	10.00	−0.4295

Table 2. Distribution of landslides for various data layers, weight of class (W$_{ij}$) of all causative factors in the study area.

Landslide Causative Factors	LSI$_{Min}$	LSI$_{Max}$	LSI$_{Range}$	LSI$_{Dev}$
Slope	−0.5723	0.8823	1.4546	−0.5183
Fault and lineament density	−3.2296	0.2835	3.5131	−1.4628
River density	−0.6478	0.5802	1.2280	−0.4851
Soil depth	−0.9763	0.2198	1.1961	−0.5453
Soil type	−0.1957	0.5277	0.7234	−0.3742
Geomorphology	−1.1850	2.2533	2.5047	−0.9107
Geology	−1.7154	0.7893	2.5047	−0.9107
Land use	−4.4242	1.0906	5.5147	−1.5015
Aspect	−1.5303	0.1484	2.1025	−0.6039

From Tables 1 and 2, it can be noted the following:

- For the slope factor, there is an obvious distinction between classes with slope angles 5–15° and >45° compared to other classes. This indicates that landslides in the study area are mainly occurring in areas with slope angles 5–15° and >45°.
- The class of fault density of 1000–1500 m/km^2 has the highest W_{ij} value (0.2835) compared to the remaining classes from all causative factors; hence, it has the highest impact on landslides in the study area.
- Cam Đường formation (W_{ij} = 0.7893) are distinctly more favorable for landslides compared to the other geological formations ($W_{ij} \leq 0.5110$).
- For the geomorphological factor, denudational and erosional slope on metamorphic rocks, Quaternary sediment, also favor landslides.
- For the land-use factor, natural reforestation land is most favorable for landslide occurrence. Other classes seem to have very little or no influence for landslides.

All W_{ij} layers for the different causative factors were constructed with QGIS 3.6 software. Next, these were summed up to obtain a resultant landslide susceptibility index map.

$$LSI = \sum_{j=1}^{n} W_{ij} \tag{2}$$

where LSI is the landslide susceptibility index and n the number of parameters.

As the result, the LSI map of Ban Khoang commune was developed and is displayed in Figure 6.
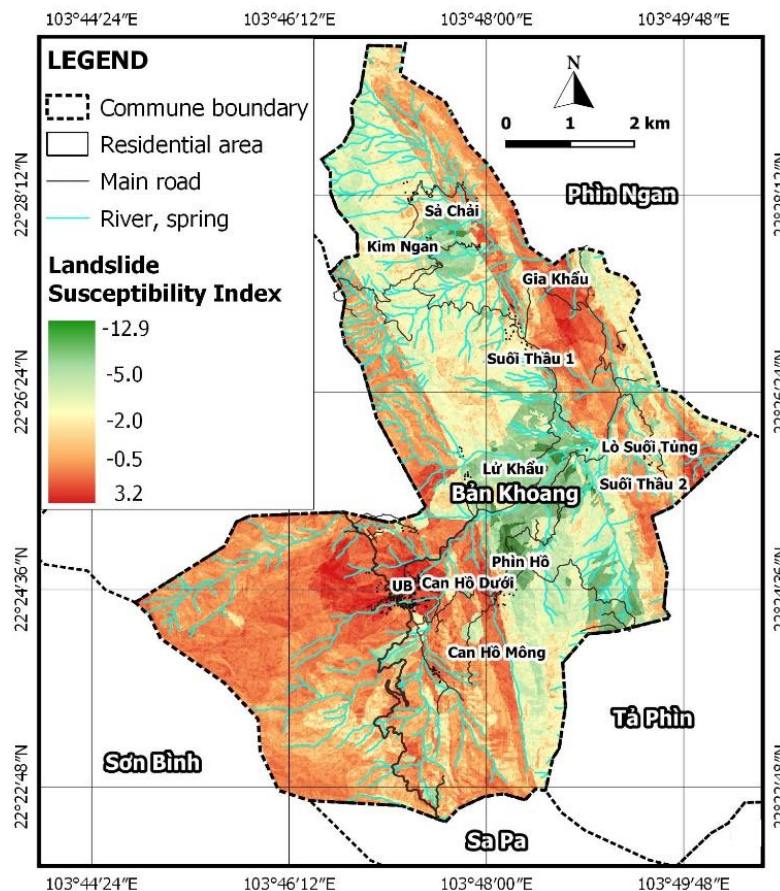
Figure 6. Map of landslide susceptibility index of Ban Khoang commune.

5. Results and Discussion

Classifier methods that have been used in landslide classification are manual classification [26,38,42–48], equal interval classification [49,50], standard deviation classification [51–55]. However, the authors usually do not explain the reasons for using a certain method in previous works.

In this study, the manual classifier method was used to reclassify the LSI values into four different susceptibility zones, according to the classification method that was proposed by Galang (2004) [56]. The susceptibility classes are low, moderate, high, and very high. Ideally, the classification method should satisfy the principle that higher landslide susceptibility classes should capture more or most landslide occurrences. Therefore, it is assumed that the expected number of observed landslide occurrences within a higher landslide susceptibility class equals two times the expected numbers in the next lower landslide susceptibility class. Hence, the expected numbers of observed landslide occurrences in the very high landslide susceptibility class equals two times the expected numbers in the high landslide susceptibility class, and so on. Based on this rule, it can be inferred that the expected percentages of observed landslide occurrences in the low, moderate, high, and very high landslide susceptibility classes are 6.7%, 13.3%, 26.7%, and 53.3% respectively.

Hence, the procedure is as follows. The landslide occurrence map is compared to the LSI map, and the cumulative percentage of observed landslide values versus ranked LSI values is calculated as shown in Figure 6. Three cut-off percentages of observed landslide occurrence in the cumulative curve are used to identify the four landslide susceptibility classes. It is 6.7% for separating the low from the moderate class, 20% for separating the moderate from high class, and 46.7% for separating the high from the very high class, as shown in Figure 7.
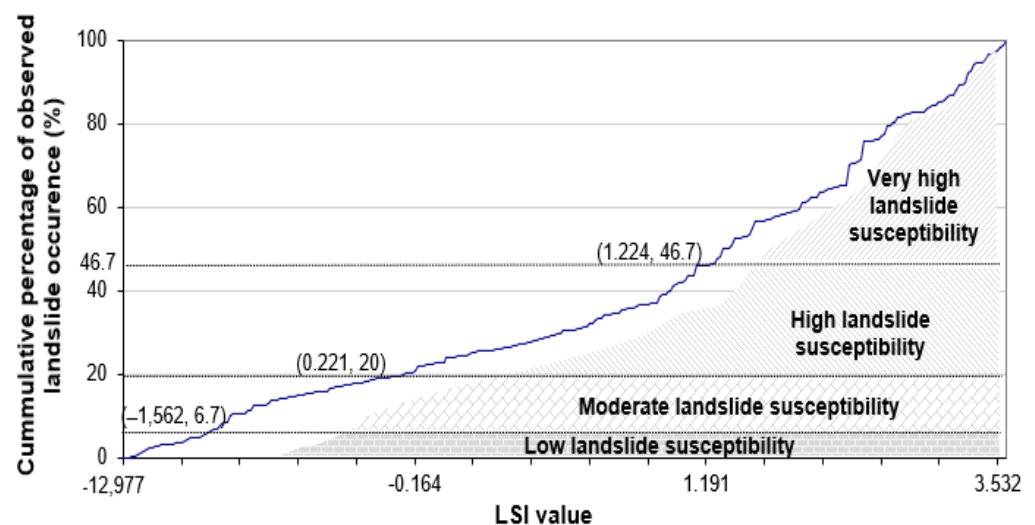
Figure 7. Cumulative percentage of observed landslide occurrence against LSI values.

As the result, the final map of landslide susceptibility zonation is shown in Figure 8. The statistical index shows that areas of low, moderate, high and very high landslide susceptibility zones are, respectively, 20.3 km^2 (38.0%), 12.4 km^2 (23.3%), 15.4 km^2 (28.9%), and 5.2 km^2 (9.8%).

In addition, to minimize the damage caused by natural disasters caused by climate change to people in Lao Cai province, Taiwan's Soil and Water Conservation Bureau (SWCB) and the Vietnam Institute of Science and Mineral Geology (VIGMR) have built a landslide monitoring station in Ban Khoang commune, Lao Cai in November 2019.
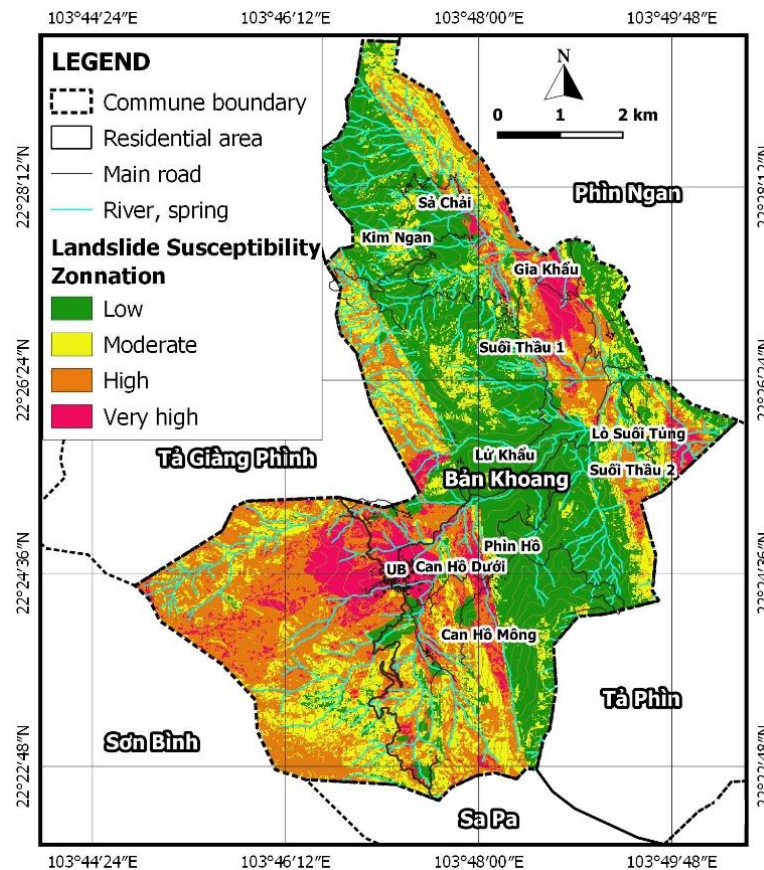
Figure 8. Map of landslide susceptibility zonation of Ban Khoang commune.

According to a survey by the VIGMR, Ban Khoang commune (Lao Cai province) is the area most at risk of landslides in Lao Cai province. At the same time, it is also the place with the highest risk of landslides in Vietnam. Therefore, installing a real-time landslide monitoring station in these two areas is essential.

Within the framework of international cooperation among the SWCB, GIS.FCU (the Geography information System Research Center of Taiwan Feng Chia University), VIGMR, WeatherPlus company (Former is AgriMedia), the projects "Study, develop a pilot debris flow early warning system in real time for mountainous areas of Vietnam" and "Study, develop a pilot debris flow early warning system in real time for mountainous areas of Vietnam" were applied to Ban Khoang area, Sa Pa town, Lao Cai province.

The real-time landslide early warning system deployed and installed in Ban Khoang includes a series of sensors, such as geophone, water level, tensiometer sensor, infrared cameras, and auto-rain gauges installed in three areas (Figure 9) (upstream (Figure 10) and midstream (Figure 11), and downstream (Figure 12)) to observe and record changes in weather conditions, such as precipitation, geology (by geogphone), hydrology (flow, water level) and the surface movement of liquid mud, soil and rock. All data are collected and processed on site (Figure 13) by the Data Processing Center.
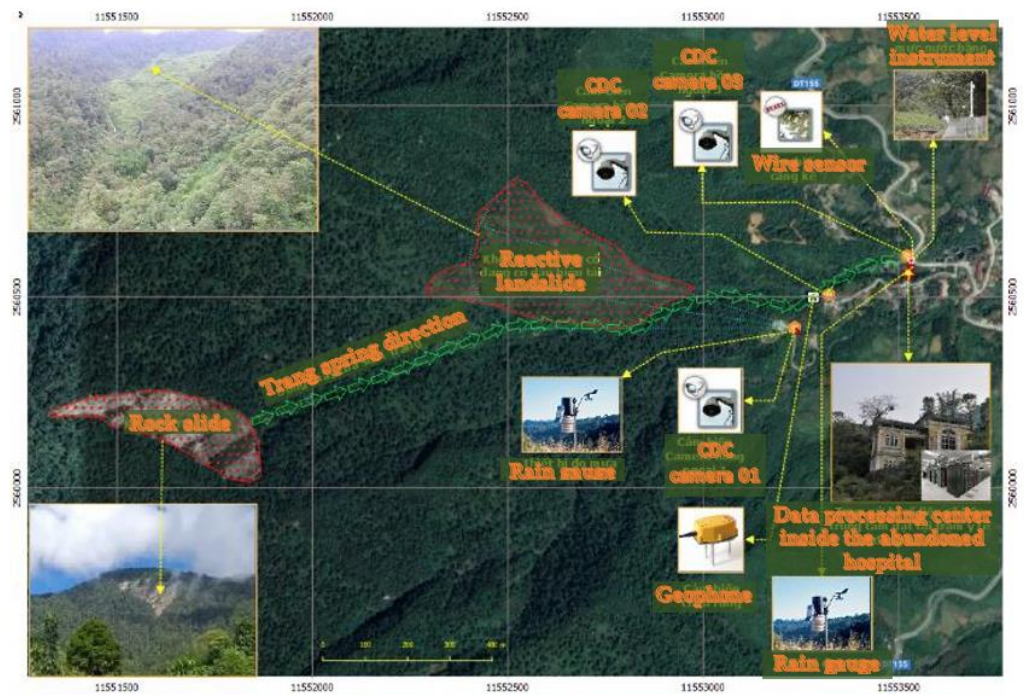
Figure 9. Real-time landslide monitoring station system in Ban Khoang, Lao Cai.

Figure 10. Upstream of the real-time landslide monitoring station.

Figure 11. Middle stream of the real-time landslide monitoring station.

Figure 12. Downstream of the real-time landslide monitoring station.

Figure 13. On-site station at the downstream of the real-time monitoring station.

6. Validation of Landslide Susceptibility Map

The final map of landslide susceptibility zonation for the study area is shown in Figure 8, and the area percentages of landslide susceptibility classes and posterior landslide susceptibility of these classes in the final LSZ map are shown in Figure 14.
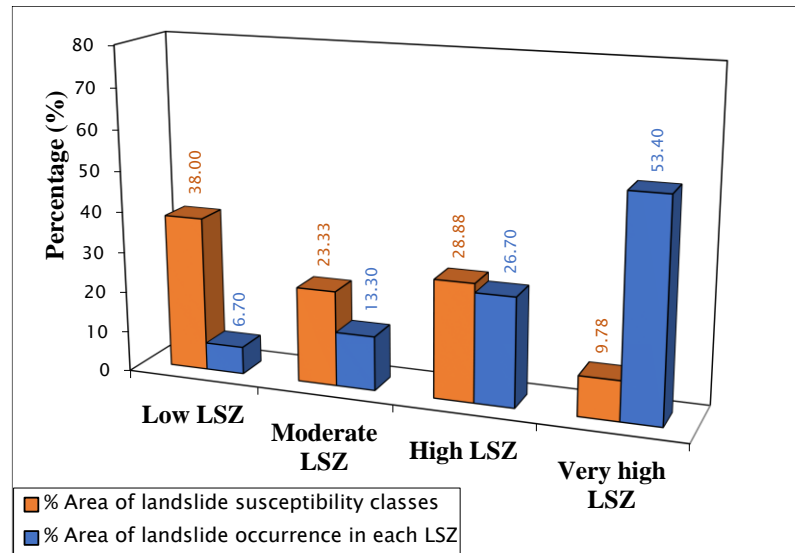
Figure 14. Area percentage of LSZ classes and the observed landslide accumulation in each LSZ class.

The accuracy of the final LSZ map is evaluated based on the observed landslides. First, Figure 13 shows that 80% observed landslide areas belonging to very high and high LSZ classes. Secondly, the final LSZ map is checked by overlaying it with the observed landslide map. In addition, As shown in Figure 14, there are various possibilities of different LSZs coinciding with a landslide polygon. Because in the inventory of the observed landslide, no distinction was made between the initiation part of the landslide and the areas of debris or flows, there can be no complete correspondence between the LSZ classes (Figure 15) that blue line is landslide area, and the complete observed landslide affected area. Hence, we consider a landslide as having "good" prediction when at least part of it is situated in a high or very high susceptibility zone. Otherwise, based on the above criteria, the model predicts 28 landslides in the study area, as shown in Table 3.

Figure 15. Example of some landslides overlaying the final LSZ map.

Table 3. LSZ validation result with observed landslide.

Accuracy of Prediction	Observed Landslide	
	Number	**Percentage (%)**
Good	22	78.57
Wrong	6	21.43

Table 3 indicates that 22 of the 28 observed landslides are well predicted (78.57%), and only 6 of the total landslides are wrongly predicted (21.43%). Figure 16 shows the LSZ map with the observed landslides indicating the different levels of prediction.
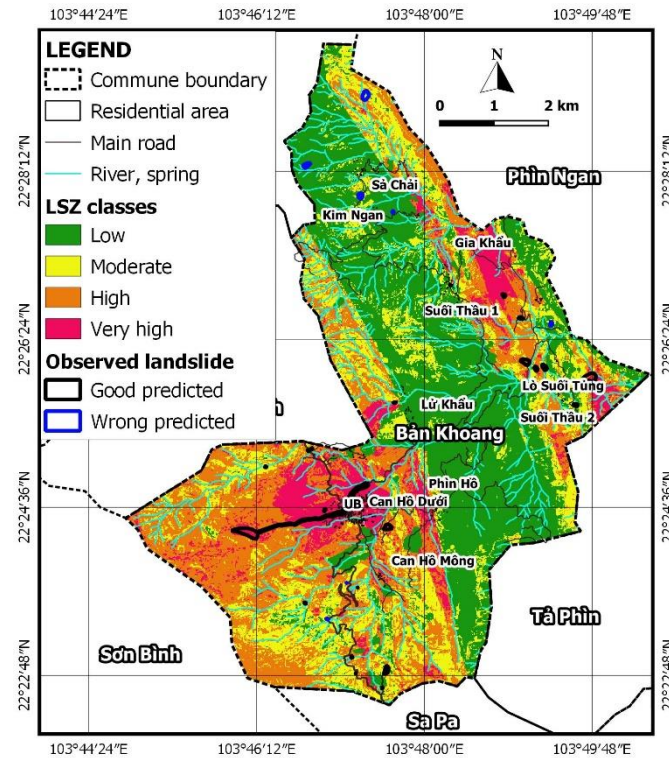
Figure 16. Validation LSZ map with observed landslides of Ban Khoang commune.

The Area Under the Curve (AUC) is used to qualitatively analyze the prediction accuracy of the landslide susceptibility map (Figure 17). The analysis results of the success rate curve indicated that the statistical index model has an approximately high AUC value of 0.803.
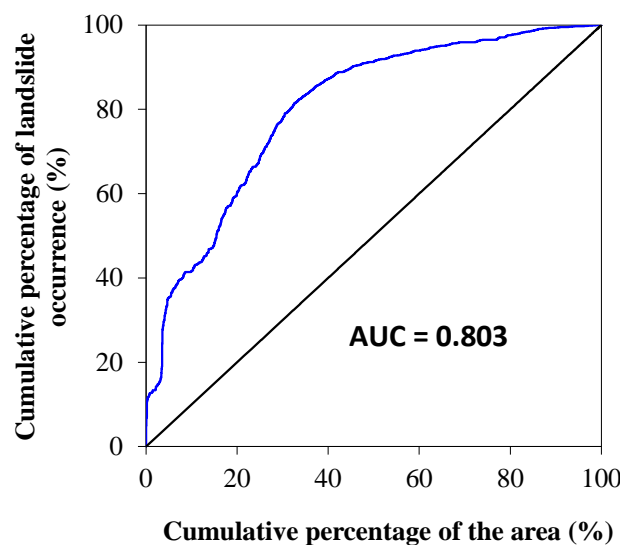
Figure 17. AUC representing quality model a success rate curve.

In terms of model performance, the accuracy of the statistical index method for landslide susceptibility mapping is approximately 80.3%, which is much closer to other studies (e.g., 74%

in the work of Conoscenti et al. (2016) [57], 71% in the work of Camilo et al. (2017) [58], 75% in the work of Youssef et al. (2015) [59], and 73.3% in the work of Shu et al. (2021) [60]). It must be admitted that this accuracy is not superior, which mainly includes the following reasons: one is that the data quality of the inventory is not very high, and the other is associated with the limitation of statistically based methods and assumptions of the landslide classification method.

Because we do not have such another area, a validation of the landslide susceptibility was performed as follows:

- A total of 75% of the observed landslides in the study area is selected at random (see Figure 18). These areas form the training data set. The actual selection was made arbitrarily without considering causative factors. It was only taken into account to spread the training data set as evenly as possible over the study area.
- On the basis of the training data set, a new LSZ map based on the statistical index method for the whole study area was created (see Figure 19).
- The remaining 25% of the observed landslides in the study area is used to evaluate the correctness of the new LSZ map.
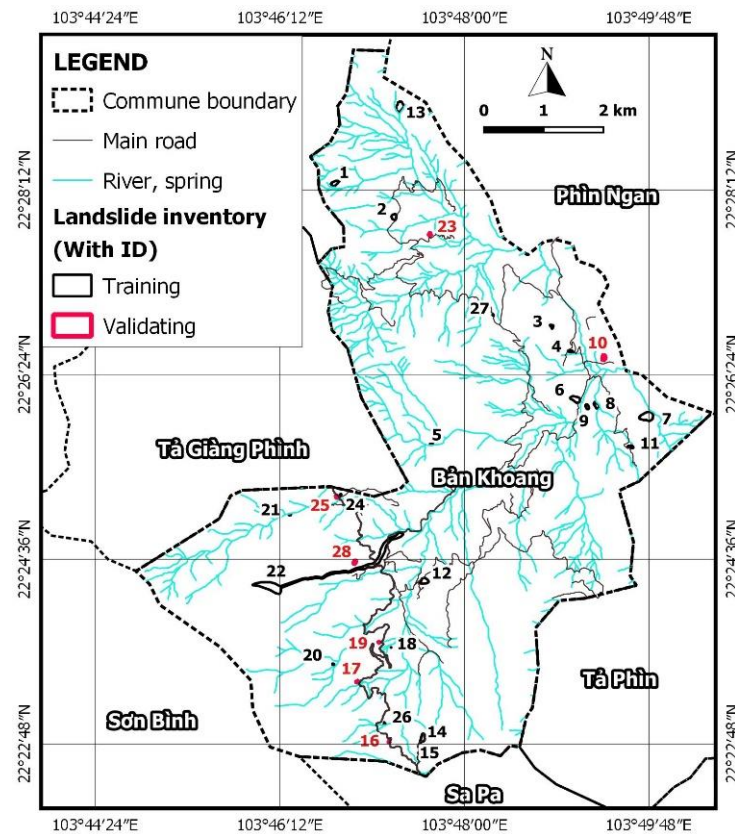
Figure 18. Randomly selected observed landslides in the study area for model validation.

It can be seen that the 80.95% of landslide number has "good" prediction for the new LSZ map based on 75% landslide training data set. Meanwhile, it is a higher value of "good" prediction (83.33%) for the landslide validating data set.
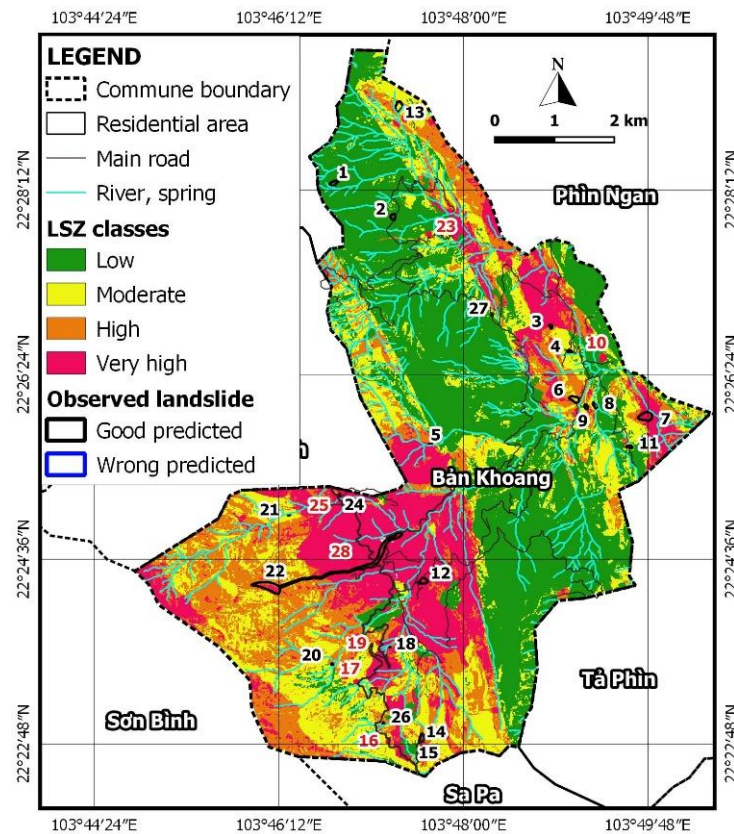
Figure 19. LSZ map based on 75% training landslides of Ban Khoang commune.

The area of landslide belonging to high and very high LSZ classes for the landslide training data set is 80%. Meanwhile the similar value for the landslide validating data set is obtained to be a little bit higher, with 81.2%. The model predictions for training and validating landslides in the study area are shown in Table 4. Generally, the results show that the target data can be predicted well with the modeling approach.

Table 4. LSZ validation result with training and validating landslide.

Accuracy of Prediction	Landslide Training Data Set				Landslide Validating Data Set			
	Number	*Percentage (%)*	*Area (km²)*	*Percentage %*	*Number*	*Percentage %*	*Area (km²)*	*Percentage %*
Wrong	4	19.05	0.0512	20	1	16.67	0.0011	18.8
Good	17	80.95	0.2050	80	6	83.33	0.0047	81.2

7. Conclusions

Because most of the observed landslides are well predicted, the high and very high landslide susceptibility classes in the final LSZ map can be considered highly believable.

For all landslides that are wrongly predicted, of course, due to the assumptions of the landslide classification method, 6.7% and 13.3% of the total observed landslide areas fall in the low and medium landslide susceptibility class, respectively. Hence, it is easy to understand that some observed landslides are not correctly predicted.

The causes of these landslides remain unanswered in this study. This probably has to do with some unique local conditions that promote landslides that were not considered in the present analyses or errors or misinterpretations of the data and factor maps.

Finally, the good prediction can be evaluated based on observed landslides belonging to very high and high LSZ classes, it can be seen that 80% observed landslide areas and 78.57% number of observed landslides were well predicted, and AUC obtained 0.803.

Hence, the LSZ map was created, and the real-time landslide monitoring station will be reliable to use in the practice.

References

1. Hoa, T.X.; Khanh, N.Q.; Ha, N.D.; Son, P.V. *Project Report of Investigation, Assessment and Geohazards Susceptibility Zonation in Mountainous Areas of VIETNAM*; Vietnam Institute of Geosciences and Mineral Resources, Ministry of Natural Resources and Environment of Vietnam: Hanoi, Vietnam, 2021.

2. Dai, F.C.; Lee, C.F. Landslide characteristics and slope instability modeling using GIS, Lantau Island, Hong Kong. *Geomorphology* **2002**, *42*, 213–228. [CrossRef]

3. Carrara, A. Multivariate models for landslide hazard evaluation. *Math. Geol.* **1983**, *15*, 403–426. [CrossRef]

4. Steger, S.; Brenning, A.; Bell, R.; Glade, T. The influence of systematically incomplete shallow landslide inventories on statistical susceptibility models and suggestions for improvements. *Landslides* **2017**, *14*, 1767–1781. [CrossRef]

5. Rossi, M.; Guzzetti, F.; Reichenbach, P.; Mondini, A.C.; Peruccacci, S. Optimal landslide susceptibility zonation based on multiple forecasts. *Geomorphology* **2010**, *114*, 129–142. [CrossRef]

6. Reichenbach, P.; Busca, C.; Mondini, A.C.; Rossi, M. The Influence of Land Use Change on Landslide Susceptibility Zonation: The Briga Catchment Test Site (Messina, Italy). *Environ. Manag.* **2014**, *54*, 1372–1384. [CrossRef] [PubMed]

7. Goetz, J.N.; Brenning, A.; Petschko, H.; Leopold, P. Evaluating machine learning and statistical prediction techniques for landslide susceptibility modeling. *Comput. Geosci.* **2015**, *81*, 1–11. [CrossRef]

8. Brenning, A. Spatial cross-validation and bootstrap for the assessment of prediction rules in remote sensing: The R package sperrorest. In Proceedings of the 2012 IEEE International Geoscience and Remote Sensing Symposium, Munich, Germany, 22–27 July 2012; pp. 5372–5375. [CrossRef]

9. Guzzetti, F.; Reichenbach, P.; Ardizzone, F.; Cardinali, M.; Galli, M. Estimating the quality of landslide susceptibility models. *Geomorphology* **2006**, *81*, 166–184. [CrossRef]

10. Frattini, P.; Crosta, G.; Carrara, A. Techniques for evaluating the performance of landslide susceptibility models. *Eng. Geol.* **2010**, *111*, 62–72. [CrossRef]

11. Cascini, L. Applicability of landslide susceptibility and hazard zoning at different scales. *Eng. Geol.* **2008**, *102*, 164–177. [CrossRef]

12. Fell, R.; Corominas, J.; Bonnard, C.; Cascini, L.; Leroi, E.; Savage, W.Z. Guidelines for landslide susceptibility, hazard and risk zoning for land use planning. *Eng. Geol.* **2008**, *102*, 85–98. [CrossRef]

13. Harp, E.L.; Keefer, D.K.; Sato, H.P.; Yagi, H. Landslide inventories: The essential part of seismic landslide hazard analyses. *Eng. Geol.* **2011**, *122*, 9–21. [CrossRef]

14. Petschko, H.; Brenning, A.; Bell, R.; Goetz, J.; Glade, T. Assessing the quality of landslide susceptibility maps—Case study Lower Austria. *Nat. Hazards Earth Syst. Sci.* **2014**, *14*, 95–118. [CrossRef]

15. Ardizzone, F.; Cardinali, M.; Carrara, A. Impact of mapping errors on the reliability of landslide hazard maps. *Nat. Hazards Earth Syst. Sci.* **2020**, *2*, 3–14. [CrossRef]

16. Galli, M.; Ardizzone, F.; Cardinali, M.; Guzzetti, F.; Reichenbach, P. Comparing landslide inventory maps. *Geomorphology* **2008**, *94*, 268–289. [CrossRef]

17. Zêzere, J.; Henriques, C.S.; Garcia, R.A.C.; Piedade, A. Effects of Landslide Inventories Uncertainty on Landslide Susceptibility Modelling; RISKam Geographical Research Centre, University of Lisbon, Lisbon, Portugal. 2009. Available online: http://eost.u-strasbg.fr/omiv/Landslide_Processes_Conference/Zezere_et_al.pdf (accessed on 20 July 2022).

18. Fressard, M.; Thiery, Y.; Maquaire, O. Which data for quantitative landslide susceptibility mapping at operational scale? Case study of the Pays d'Auge plateau hillslopes (Normandy, France). *Nat. Hazards Earth Syst. Sci.* **2014**, *14*, 569–588. [CrossRef]

19. Long, N.T. *Landslide Susceptibility Mapping of the Mountainous Area in a Luoi District, Thua Thien Hue Province, Vietnam*; Faculty of Engineering, Department of Hydrology and Hydraulic Engineering, Vrije Universiteit Brussel: Brussel, Belgium, 2008.

20. Van Westen, C. Statistical Landslide Hazard Analysis. In *ILWIS 2.1 for Windows Application Guide*; ITC Publication: Enschede, The Netherlands, 1997; pp. 73–84.

21. Berhane, G.; Tadesse, K. Landslide susceptibility zonation mapping using statistical index and landslide susceptibility analysis methods: A case study from Gindeberet district, Oromia Regional State, Central Ethiopia. *J. Afr. Earth Sci.* **2021**, *180*, 104240. [CrossRef]

22. Mandal, S.; Mandal, K. Bivariate statistical index for landslide susceptibility mapping in the Rorachu river basin of eastern Sikkim Himalaya, India. *Spat. Inf. Res.* **2018**, *26*, 59–75. [CrossRef]

23. Wu, Z.; Wu, Y.; Yang, Y.; Chen, F.; Zhang, N.; Ke, Y.; Li, W. A comparative study on the landslide susceptibility mapping using logistic regression and statistical index models. *Arab. J. Geosci.* **2017**, *10*, 187. [CrossRef]

24. Wang, Q.; Li, W.; Wu, Y.; Pei, Y.; Xie, P. Application of statistical index and index of entropy methods to landslide susceptibility assessment in Gongliu (Xinjiang, China). *Environ. Earth Sci.* **2016**, *75*, 1–13. [CrossRef]

25. Bui, D.T.; Lofman, O.; Revhaug, I.; Dick, O. Landslide susceptibility analysis in the Hoa Binh province of Vietnam using statistical index and logistic regression. *Nat. Hazards* **2011**, *59*, 1413–1444. [CrossRef]

26. Oztekin, B.; Topal, T. GIS-based detachment susceptibility analyses of a cut slope in limestone, Ankara—Turkey. *Environ. Earth Sci.* **2005**, *49*, 124–132. [CrossRef]

27. Cevik, E.; Topal, T. GIS-based landslide susceptibility mapping for a problematic segment of the natural gas pipeline, Hendek (Turkey). *Environ. Geol.* **2003**, *44*, 949–962. [CrossRef]

28. Guzovski, L.A.; Toản, T.X.; Hiến, P.Đ. Some Problems of Study on the Weathering Crust in South Vietnam. *Geol. Miner. Resour.* **1989**, *2*, 29–36.

29. An, P.V.; Bính, H.V.; Hiền, L.V.; Phú, Đ.X.; Dũng, N.T. Geochemical charateristics of the tropical humid weathering crust in Vietnam. *Geol. Miner. Resour. J.* **1990**, *3*, 95–104.

30. Sarkar, S.; Kanungo, D.P.; Mehrotra, G.S. Landslide hazard zoning: A case study in Garhwal Himalaya, India. *Mt. Res. Dev.* **1995**, *15*, 301–309. [CrossRef]

31. Sidle, R.C.; Ochiai, H. *Landslides: Processes, Prediction, and Land Use*; Water Resources Monograph No.18; American Geophysical Union: Washington, DC, USA, 2006; 312p.

32. Lap, D.Q.; Binh, D.T.; Loc, N.V.; Son, P. *Map of Geology and Mineral Resources of Lao Cai Sheet Group, Scale 1:50,000*; Intergeo Geological Section; MONRE: Hanoi, Vietnam, 2003.

33. Thành, N.Q.; Dung, N.P.; Hoàng, N.V.; Hiến, T.T. *Study for Assessments of Landslide, Debris flow and Flash Flood in Focused Area of Lao Cai Province (Districts of Bat Xat & Sa Pa and Lao Cai city) and Propose Remedy Damage Solutions (Branch Project Belonging to National Project KC 01-08)*; Hanoi, Vietnam, 2006.

34. Chigira, M.; Nakamoto, M.; Nakata, E. Weathering mechanisms and their effects on the landsliding of ignimbrite subject to vapor-phase crystallization in the Shirakawa pyroclastic flow, northern Japan. *Eng. Geol.* **2002**, *66*, 111–125. [CrossRef]

35. Wakatsuki, T.; Tanaka, Y.; Matsukura, Y. Soil slips on weathering-limited slopes underlain by coarse-grained granite or fine-grained gneiss near Seoul, Republic of Korea. *CATENA* **2005**, *60*, 181–203. [CrossRef]

36. Ibetsberger, H.J. The Tsergo Ri landslide: An uncommon area of high morphological activity in the Langthang valley, Nepal. *Tectonophysics* **1996**, *260*, 85–93. [CrossRef]

37. Pachauri, A.K.; Gupta, P.V.; Chander, R. Landslide zoning in a part of the Garhwal Himalayas. *Environ. Earth Sci.* **1998**, *36*, 325–334. [CrossRef]

38. Gökceoglu, C.; Aksoy, H. Landslide susceptibility mapping of the slopes in the residual soils of the Mengen region (Turkey) by deterministic stability analyses and image processing techniques. *Eng. Geol.* **1996**, *44*, 147–161. [CrossRef]

39. Gokceoglu, C. Discussion on "Landslide hazard zonation of the Khorshrostam area, Iran" by A. Uromeihy and M.R. Mahdavifar. *Bull. Eng. Geol. Environ.* **2001**, *58*, 207–213.

40. Greenway, D.R. Vegetation and slope stability. In *Slope Stability, Geotechnical Engineering and Geomorphology*; Anderson, M.G., Richards, K.S., Eds.; John Wiley & Sons: Chichester, UK, 1987; pp. 187–230.

41. Land Administration Department of the Ministry of Natural Resources and Environment. *Landuse Map of Lao Cai Province, Scale 1:50,000*; Land Administration Department of the Ministry of Natural Resources and Environment: Hanoi, Vietnam, 2019.

42. Yalcin, A. GIS-based landslide susceptibility mapping using analytical hierachy process and bivariate statistics in Ar-desen (Turkey). *Catena* **2007**, *72*, 1–12. [CrossRef]

43. Van Westen, C.J.; Rengers, N.; Terlien, M.T.J.; Soeters, R. Prediction of the occurrence of slope instability phenomena through GIS-based hazard zonation. *Geol. Rundsch.* **1997**, *86*, 404–414. [CrossRef]

44. Binaghi, E.; Luzi, L.; Madella, P.; Pergalani, F.; Rampini, A. Slope Instability Zonation: A Comparison Between Certainty Factor and Fuzzy Dempster–Shafer Approaches. *Nat. Hazards* **1998**, *17*, 77–97. [CrossRef]

45. Barredo, J.; Benavides, A.; Hervás, J.; van Westen, C.J. Comparing heuristic landslide hazard assessment techniques using GIS in the Tirajana basin, Gran Canaria Island, Spain. *Int. J. Appl. Earth Obs. Geoinform.* **2000**, *2*, 9–23. [CrossRef]

46. David, J.W.; Paul, F.H. Mapping landslide susceptibility in Travis County, Texas, USA. *Geol. J.* **2000**, *51*, 245–253.

47. Saha, A.K.; Gupta, R.P.; Arora, M.K. GIS-based Landslide Hazard Zonation in the Bhagirathi (Ganga) Valley, Himalayas. *Int. J. Remote Sens.* **2002**, *23*, 357–369. [CrossRef]

48. Lan, H.; Zhou, C.; Wang, L.; Zhang, H.; Li, R. Landslide hazard spatial analysis and prediction using GIS in the Xiaojiang watershed, Yunnan, China. *Eng. Geol.* **2004**, *76*, 109–128. [CrossRef]

49. Lee, C.F.; Li, J.; Xu, Z.W.; Dai, F.C. Assessment of landslide susceptibility on the natural terrain of Lantau Island, Hong Kong. *Environ. Earth Sci.* **2001**, *40*, 381–391. [CrossRef]

50. Kanungo, D.; Arora, M.; Sarkar, S.; Gupta, R. A comparative study of conventional, ANN black box, fuzzy and combined neural and fuzzy weighting procedures for landslide susceptibility zonation in Darjeeling Himalayas. *Eng. Geol.* **2006**, *85*, 347–366. [CrossRef]

51. Ayalew, L.; Yamagishi, H.; Ugawa, N. Landslide susceptibility mapping using GIS-based weighted linear combination, the case in Tsugawa area of Agano River, Niigata Prefecture, Japan. *Landslides* **2004**, *1*, 73–81. [CrossRef]

52. Akgün, A.; Bulut, F. GIS-based landslide susceptibility for Arsin-Yomra (Trabzon, North Turkey) region. *Environ. Earth Sci.* **2006**, *51*, 1377–1387. [CrossRef]

53. Mehmet, L.S.; Vedat, D. A comparison of the GIS based landslide susceptibility assessment methods: Multivariate versus bivariate. *Environ. Geol.* **2004**, *45*, 665–679. [CrossRef]

54. Komac, M. A landslide susceptibility model using the Analytical Hierarchy Process method and multivariate statistics in perialpine Slovenia. *Geomorphology* **2006**, *74*, 17–28. [CrossRef]

55. Foumelis, M.; Lekkas, E.; Parcharidis, I. Landslide susceptibility mapping by GIS-based qualitative weighting pro-cedure in Corinth area. Bulletin of 10th International Congress of the Geological Society. *Thessalloniki* **2004**, *34*, 904–912.

56. Galang, J.S. A Comparison of GIS Approaches to Slope Instability Zonation in the Central Blue Ridge Mountains of Virginia. Master's Thesis, Faculty of Virginia Polytechnic Institute and State University, Blacksburg, Virginia, 2004; 99p.

57. Conoscenti, C.; Rotigliano, E.; Cama, M.; Caraballo-Arias, N.A.; Lombardo, L.; Agnesi, V. Exploring the effect of absence selection on landslide susceptibility models: A case study in Sicily, Italy. *Geomorphology* **2016**, *261*, 222–235. [CrossRef]

58. Camilo, D.C.; Lombardo, L.; Mai, P.M.; Dou, J.; Huser, R. Handling high predictor dimensionality in slope-unit-based landslide susceptibility models through LASSO-penalized Generalized Linear Model. *Environ. Model. Softw.* **2017**, *97*, 145–156. [CrossRef]

59. Youssef, A.M.; Al-Kathery, M.; Pradhan, B. Landslide susceptibility mapping at Al-Hasher area, Jizan (Saudi Arabia) using GIS-based frequency ratio and index of entropy models. *Geosci. J.* **2015**, *19*, 113–134. [CrossRef]

60. Shu, H.; Guo, Z.; Qi, S.; Song, D.; Pourghasemi, H.R.; Ma, J. Integrating Landslide Typology with Weighted Frequency Ratio Model for Landslide Susceptibility Mapping: A Case Study from Lanzhou City of Northwestern China. *Remote Sens.* **2021**, *13*, 3623. [CrossRef]